ISSN 0915-633X

NATIONAL INSTITUTE FOR FUSION SCIENCE

Multibarrel Repetitive Injector with a Porous Pellet Formation Unit

I. Viniar and S. Sudo

(Received - July 9, 1997)

NIFS-501 July 1997

RESEARCH REPORT
NIFS Series

NAGOYA, JAPAN

MULTIBARREL REPETITIVE INJECTOR WITH A POROUS PELLET FORMATION UNIT

I. Viniar and S. Sudo*

Saint-Petersburg State Technical University
29, Politechnitcheskaya, Saint-Petersburg, 195251, RUSSIA,

***National Institute for Fusion Science, 322-6, Oroshi-cho, Toki, Gifu, 509-52, JAPAN**

ABSTRACT

New repetitive multibarrel pellet injector for steady-state fueling and diagnostics purposes in large fusion devices has been designed. The injector is intended to apply in the Large Helical Device at the National Institute for Fusion Science in Japan. The steady-state operation is provided by ten pipe-guns with unique porous units forming solid hydrogen pellets for 5 - 9 s in every barrel. Over one thousand hydrogen pellets have been formed and accelerated to 1.2 km/s at the different repetitive rates. The injector design and experimental results are presented.

Keywords: hydrogen pellet, pellet injector, fueling, pipe gun, porous block

1. INTRODUCTION

One of the basic missions of Large Helical Device (LHD), under construction at National Institute for Fusion Science in Japan, is to demonstrate a steady-state operation of helical system. Plasma control is one of the key subjects for the LHD successful operation. The powerful technique for plasma density and pressure profiles controlling is a pellet injection. The pellet injection is also intended for refueling particles in the plasma core and plasma diagnostics. Therefore, an adequate pellet injection system for LHD should be developed. Its basic parameters, presented in [1], should be demonstrated before steady-state operation mode start.

The basic features of a pellet injector for LHD should be fixed as follows:

- high reliability, which should be checked by the long time of the injector exploitation;
- high flexibility in changing of a long term operation, including steady-state injection mode, an injection interval, depth penetration, deposited particles number and others.

New pellet production technology was proposed [2] and successfully tested at NIFS in 1994 [3,4] . Recently ten barrels pellet injector, based on this technology and presented in this report, was designed for satisfaction of all LHD requirements, including fueling at the steady-state operation. Section 2 presents a description of the proposed pellet injector design. The achieved experimental results are presented in Sec. 3. Conclusion is given in Sec. 4.

2. PELLET INJECTOR DESIGN

The multibarrel pellet injector MPI-10 is intended to fire by an unlimited number of solid hydrogen or deuterium pellets from every barrel at the repetitive steady-state mode. Every barrel is able to inject pellets independently of others and to stay in a 'stand by' mode also. A pellet mass and velocity can be measured and the pellet shape in flight can be recorded by a video recorder with a CCD-camera. MPI-10 is able to operate both at automatic and at manual modes.

The principle of pellet production by means of the new technology are described in [2-4]. Pure H_2 or D_2 at room temperature is being admitted continuously into a gun barrel through a porous sleeve being maintained at the temperature below the melting point of the fuel (See Fig. 1). A portion of liquid (or fluid) fuel is frozen there forming a pellet. This state is stable, and the pellet can wait for an injection moment for a long time. Then the propellant high-pressure gas is admitted in the barrel for a 1-10 ms to accelerate the frozen pellet and it heats the porous sleeve also. The solid fuel inside the sleeve is heated up to the melting point and penetrates into the barrel. New portions of fuel gas are cooled and frozen inside the porous sleeve replenishing the fuel consumption. Liquid (or fluid solid) fuel is frozen inside the gun barrel forming a new pellet. The cycle can be repeated.

The MPI-10 consists of ten pipe-guns with ten independent cryogenic pellet formation units, cooling by liquid helium, a diagnostic chamber equipped with laser, a photodetector with an amplifier, an optical fiber, a differential vacuum pumping system with guide tubes, a vacuum pumping system, a control rack with a logic controller for automatic (or manual) remote control, a microwave pellet mass detector. The schematic diagram of the MPI-10 is presented in Fig. 2.

Ten independently operating porous pipe-guns are housed inside a vacuum chamber in two rows, five units in a line. Every pipe-gun is equipped with a fast propellant gas valve, a fuel gas valve, a vacuum gate valve, a porous pellet formation unit with a cryogenic heat exchanger and a logic controller. The inner barrels diameters are 1.5mm , 2mm, 2.7mm, 3mm

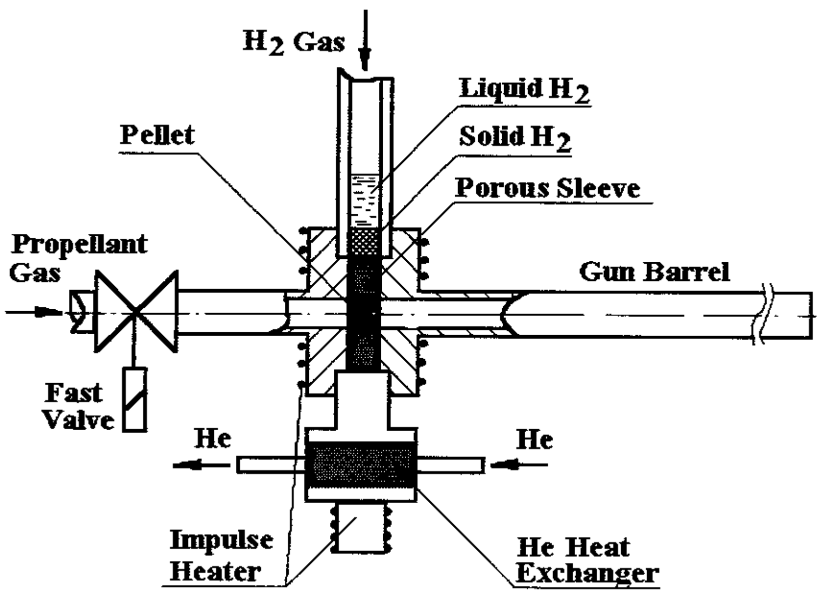

Fig. 1. Schematic of the injector with a porous pellet formation unit

and 3.8 mm for every pair barrels. Their lengths are 370 mm and 420 mm. The porous unit is equipped with a thermal sensor and a heater. The cooling helium vapor is admitted from a Dewar vessel, penetrates through every ten heat exchangers and removed through a coaxial slit between the inlet and outlet tubes.

All fast and fuel valves are attached to the cryostat vacuum chamber flange. Four vacuum connectors for temperature gauges and heaters are placed on this flange also. There are two identical aluminum blocks with five gate valves in each. Five stainless steel plates moves for 3-5 ms between every five pair Teflon gaskets by means of electromagnets inside every aluminum block. There are holes in the plates for the pellet coming through. The blocks are attached to the other cryostat vacuum chamber flange. The diagnostic chamber with two pair of windows is attached to the opposite side of the gate valves blocks. First two windows having ∅ 80 mm is used for pellet registration by laser and photodetector. Second two windows ∅ 220 mm is used for recording pellets in flight by a video recorder with CCD-camera and a nanopulse flash. The diagnostic chamber is able to rotate and fix in any position. The ends of the guide tubes are inserted into the diagnostic chamber (not shown in Fig. 2). The other guide tubes ends are inserted into high vacuum chamber for pellet mass measurement (not shown in Fig. 2).

The pellet formation unit is made of a pure copper block with a porous sleeve inside, as shown in Fig. 3. The helium heat exchanger is manufactured inside the below part of the block. The heater from a manganine wire (18 Ohm) is wrapped around the upper part of the block. Porous sleeve (∅ 10 mm) is made from several copper meshes with holes equaled to the barrel inner diameter on the axis. The meshes are pressed inside the copper block up to the thickness of 3 mm. The barrel and a tube fitted to the fast valve are hermetically attached from both opposite sides to the porous block by indium gaskets . Fuel gas is able to penetrate inside the meshes through a hole in the upper part of the copper block. All cryogenic parts are housed inside a radiation screen made from copper.

The fuel gas supply system consists of a gas collector with one vacuummeter and ten outlets for every fuel valve, connected with the pellet formation unit inlet tubes. Fuel gas is admitted to the gas collector from a standard cylinder with a reducer. A collector for the

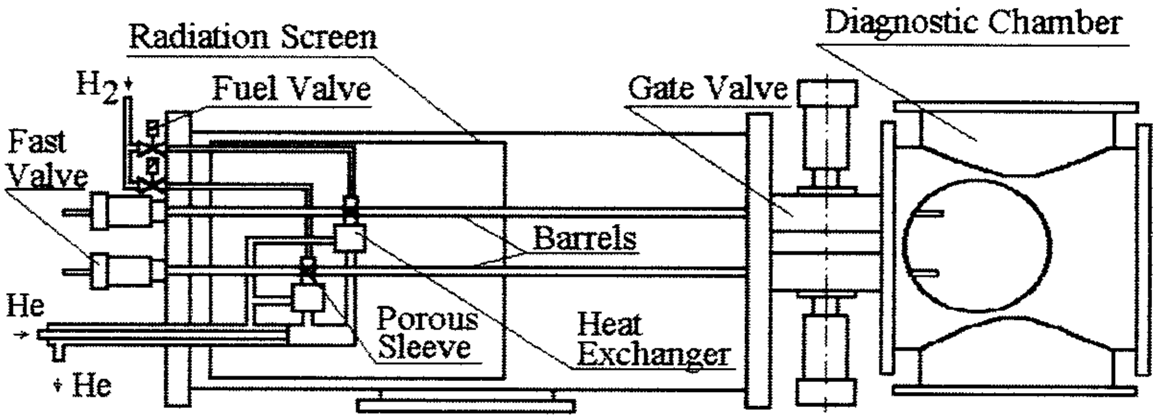

Fig. 2. Schematic diagram of the repetitive multibarrel pellet injector

propellant gas supply system has ten independent channels, connected to a cylinder with high pressure gas. Ten pressure gauges can be attached to every independent channels. The fast valve is a pilot type electromagnetic valve with polyimide gasket and open/close cycle near 1 ms. A work volume inside the valve is approximately 6cm^3.

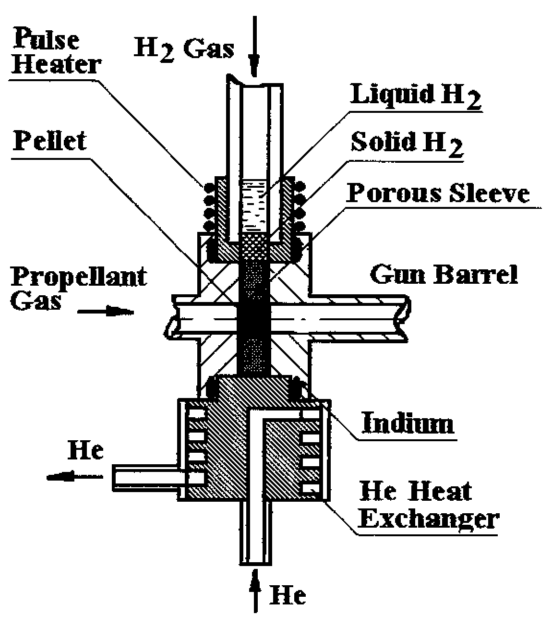

Fig. 3. Schematic diagram of the porous pellet formation unit

Cryogenic and pellet mass measuring chambers are pumped by two turbomolecular pumps with 500 l/s evacuating ability. Diagnostic and intermediate chambers of differential pumping system are pumped by rotor pumps. All chambers are equipped by high vacuum and Pirani gauges.

3. PELLET INJECTOR OPERATION AND EXPERIMENTAL RESULTS

The cryogenic and other vacuum chambers are pumped out up to 10^{-2}-10^{-4} Pa. All valves, including the gate valves are in open positions. The fuel and propellant gas supply systems are pumped also and filled by pure gases. Helium vapor from a Dewar vessel cools the cryogenic parts of the injector. The temperature of the porous units achieves of 8-9 K in a 60-100 minutes in dependence of pressure into the Dewar vessel. The control rack is switched on and the injector is ready for the pellet injection.

The basic aim of the first stage of experiments was to minimize the cycle time of a pellet formation and injection from one barrel. There was produced the injector for ten barrels, but only four injection channels were assembled with the porous formation units, which were differed by different dimensions and designs. All experiments and pellet injector tests were carried out with these units in turn for one barrel only. The results are presented below in case of operation with hydrogen for clear demonstration. Some negligible differs were observed with deuterium.

There are two operation modes for the proposed pellet injector: 'liquid' and 'solid'. In case of 'liquid' mode the porous pellet formation unit should be heated to the temperature exceeding the triple point of the fuel (14 K for hydrogen and 18 K for deuterium). Liquid fuel penetrates into the barrel and forms a pellet. In case of 'solid' mode the porous pellet formation unit should be heated lower fuel triple point. In these conditions the fluid solid fuel is pushed through the porous sleeve into the barrel and forms a pellet also. The both operation modes can be realized in the same pellet formation unit design. The powerful of the addition heater attached to the pellet formation unit should be changed in these modes only. The operation parameters of the injector units are different in these modes also, of course.

3.1. 'Liquid' mode

The schematic diagram of the operating pulses in this mode is shown in Fig. 4. These pulses are formed in the logic controller, which initiates the pellet injection as at a single shot, and at the repetitive mode also. The logic controller allows to adjust the optimal cycle parameters before starting in wide intervals for the different pellet formation unit designs. The presented below cycle parameters corresponds with the pellet injection time of 8.9 s for the porous unit mass of 77 g.

The cycle starts by a pulse of the propellant gas, which is admitted from the fast valve. Propellant gas comes out from the barrel for 80 ms and the gate valve is closed. Heater is switched on for 0.8 s after the fast valve pulse with time delay of 10 ms. The porous unit accumulates near 8 J heat from the heater. The frozen hydrogen inside the porous unit is melted and penetrates into the barrel for 1-2 s. The typical thermal sensor signals of the process are shown in Fig. 5. During experiment the fuel valve was opened all time of operation. Liquid hydrogen inside the small porous cells has frozen for 1-2 s and after that the addition portions of liquid hydrogen could not penetrate into the barrel. The porous unit worked as a 'heat valve'. The hydrogen gas pressure above the porous unit was equaled to 0.1 MPa. Liquid hydrogen inside the barrel is frozen and cooled to 8-9 K for 5-6 s. This was the longest period of the pellet formation time. Then the gate valve has been opened and the next shot has been done by a fast valve after 0.9 s. Propellant gas and pellet originated gas are evacuated by forevacuum pump. The cycle has been repeated. The minimum duration of the whole cycle was registered of 8.9 s. The pellet formation process and cycle duration have been recorded by a CCD-camera. The pellet velocities above 1 km/s have been achieved with the initial helium propellant gas pressure of 6 MPa. The typical pellet shape is shown in Fig. 6.

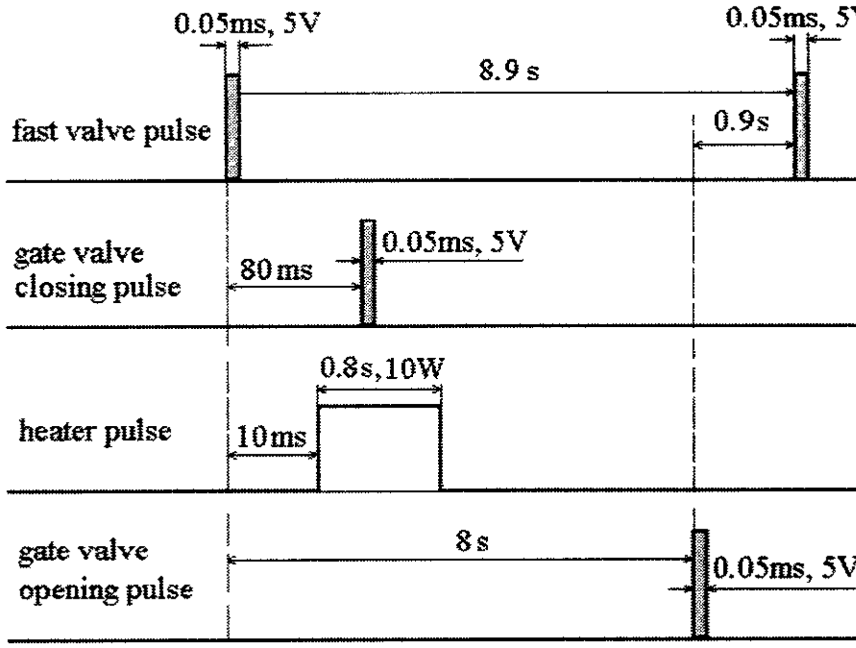

Fig. 4. Schematic diagram of the pulses during a pellet injection cycle at the 'liquid' mode

The pellet diameter is 2.4 mm and length is between 3 mm and 4 mm. The pellet diameter reduction in comparison with the barrel diameter of 2.7 mm is about 10%. This reduction is usual for solid hydrogen pellet injection in other injectors [5,6]. To reduce the pellet formation time, some improvements in porous unit design should be done. A mathematical model of the optimal pellet formation process is developing now. First estimations predict the minimum pellet formation time near 1 s at this mode. Attempts to reduce the pellet formation time in this 77 g porous unit led to the pellet destruction. The pellet had not enough time for freezing and its central part along the axis had a snow area, as shown in Fig. 7. Such pellets were often destroyed during the injection.

Over 1000 pellets have been formed and injected during several series in this mode with small intervals between series. Some results of the pellet registration during these series under the different cycle times are shown in Table 1. The pellet injection reliability is calculated as a ratio of good quality injected pellet to all pellets in series. A series of pellets from number C545 to C555 at the rate of one shot per 9 s from single barrel is presented in Fig. 8.

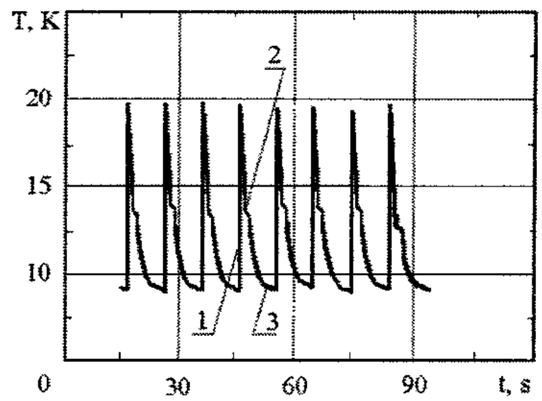

Fig. 5. The typical thermal sensor signals of the pellet formation and shooting process at the 'liquid' mode:
1-shooting; 2-solid hydrogen melting and barrel filling by liquid;
3 - pellet freezing.

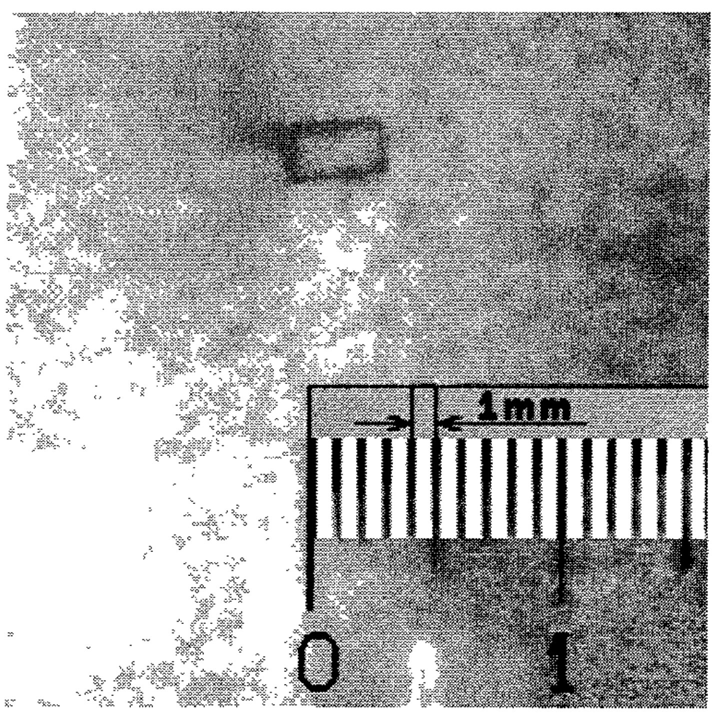

Fig. 6. A hydrogen pellet in flight.

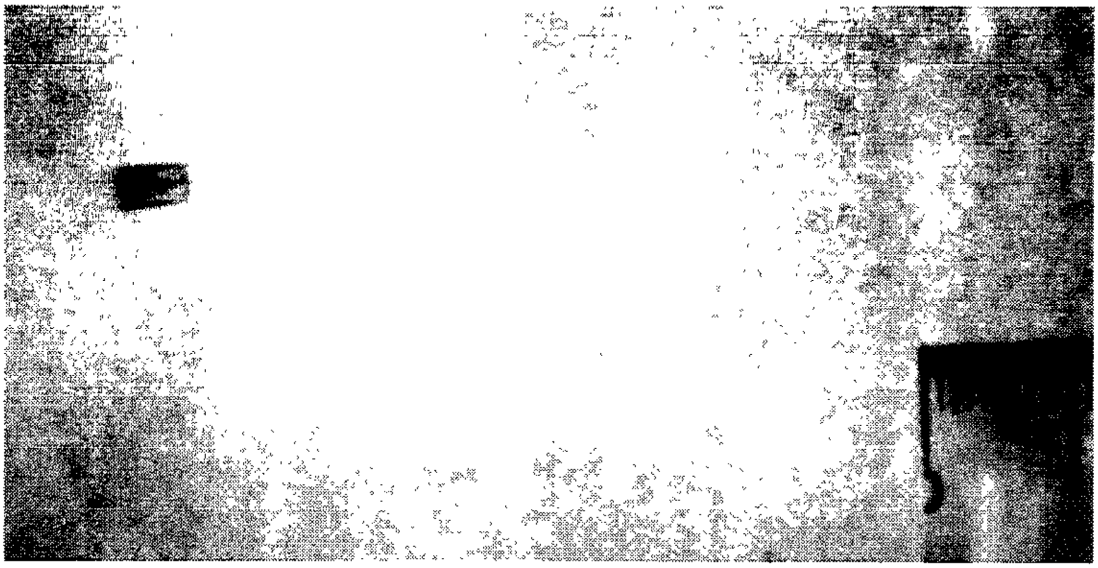

Fig. 7. A defect hydrogen pellet in flight:
There is a snow area along the pellet axis which can lead to its destruction.

Table 1. Series of hydrogen pellets injected at the 'liquid' and the 'solid' modes.

Amount of pellets in series	Injection cycle time	Amount of good quality pellets in series	Injection reliability
'LIQUID' MODE			
15	9 s	10	67%
26	9 s	16	62%
55	9 s	33	60%
22	10 s	14	64%
26	11 s	19	73%
25	15 s	17	68%
25	19 s	21	87%
23	19 s	20	87%
47	19 s	36	77%
'SOLID' MODE			
12	5 s	11	92%
17	6 s	13	76%
25	6 s	22	88%
13	7 s	12	92%

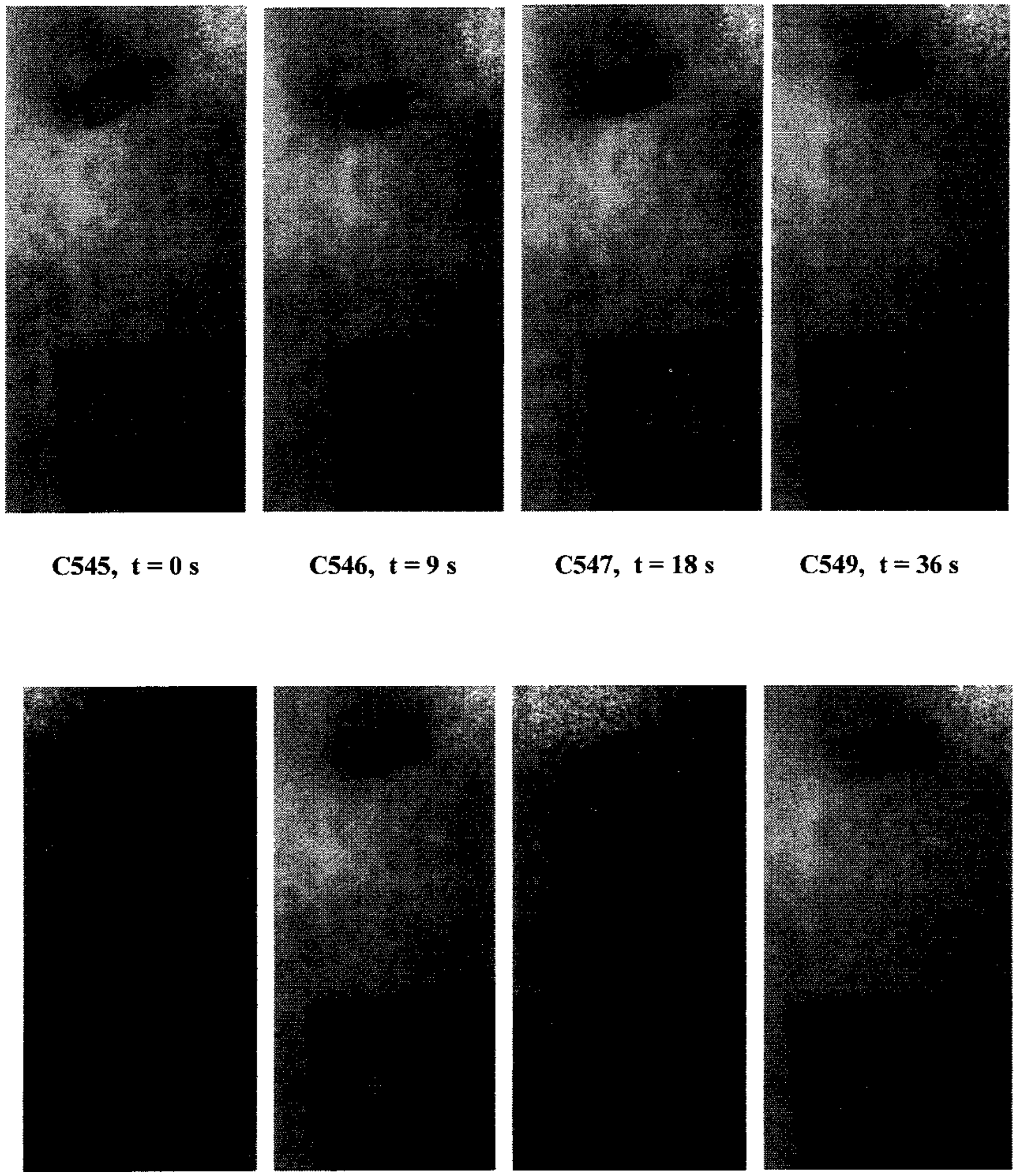

Fig. 8. A series of the solid hydrogen pellets in flight at the injection rate of 1 shot per 9 s.

3.2. 'Solid' mode

The schematic diagram of the operating pulses in this mode is shown in Fig. 9. These pulses are formed in the logic controller also. The presented below cycle parameters corresponds with the pellet injection time of 6 s for the porous unit mass of 30 g.
The cycle starts by a pulse of the propellant gas, which is admitted from the fast valve. Propellant gas comes out from the barrel for 80 ms. Heater is switched on for 0.4 s after the fast valve pulse with time delay of 10 ms. The porous unit accumulates near 4 J heat from the heater and it is heated to 14 K. The fluid solid hydrogen inside the porous unit is pushed out into the barrel for less than 1 s by hydrogen gas pressure of 3 MPa maintained above the porous unit. Solid fluid hydrogen inside the porous cells cools to 12-13 K for less than 1 s and after that the addition portions of fluid hydrogen can not penetrate into the barrel. The porous unit worked as a 'heat valve' at this mode also. Fluid hydrogen inside the barrel is cooled to 9-10 K for 3-5 s. This was the longest period of the pellet formation time. Next shot has been done by a fast valve every 6 s. Propellant gas and pellet originated gas are evacuated by the forevacuum pump. The cycle is repeated. The typical thermal sensor signals of the process are shown in Fig. 10. During experiment the gate valve and the fuel valve were opened all time of operation. The minimum duration of the whole cycle was registered of 5 s. Some modification of the fast valve power supply unit should be done to reduce the cycle time. The pellet formation process and cycle duration have been recorded by a CCD-camera. The pellet velocities above 1 km/s have been achieved with the initial helium propellant gas pressure of 6 MPa. Over 100 pellets have been formed and injected during several series in this mode with small intervals between series. Some results of the pellet registration during these series under the different cycle times are shown in Table 1 also. The pellet injection reliability is calculated as a ratio of unbroken pellets to all pellets in series. The typical pellet shape is shown in Fig. 11. The pellets had not transparent shape, because the fluid solid hydrogen was extruded through the porous unit in the form of many ice threads. Such pellet is a polycrystal, but rather strong to be accelerated above 1 km/s. The pellet injection of such pellets in fusion devices must prove their ability to deliver fuel in a core area of plasmas. The estimations predict the pellet injection cycle time less than 1 s at this mode.

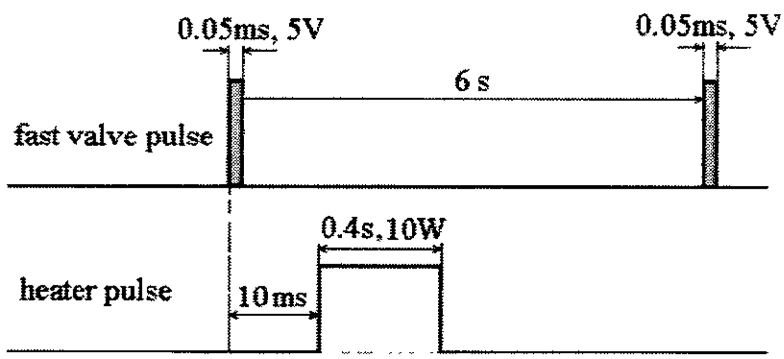

Fig. 9. Schematic diagram of the pulses during a pellet injection cycle at the 'solid' mode

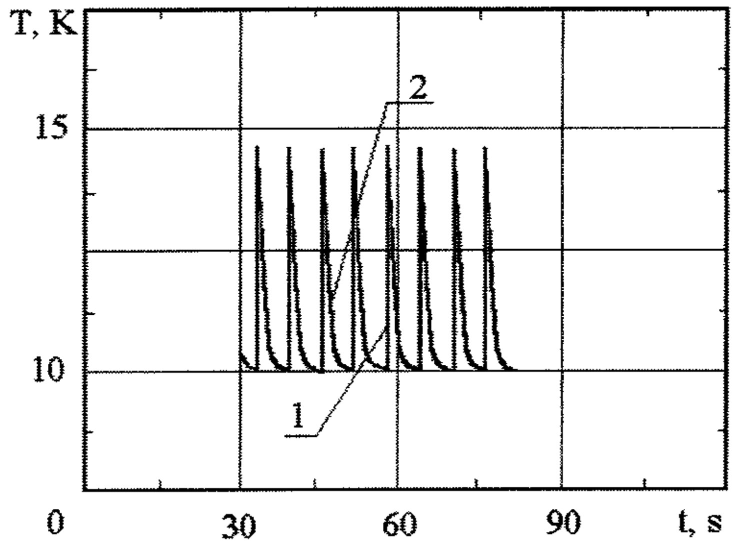

Fig. 10. The typical thermal sensor signals of the pellet formation and shooting process at the 'solid' mode:
1 - shooting and heating; 2 - barrel filling by solid fluid hydrogen.

3.3. 'Stand By' mode

A 'stand by' mode can be initiated at any moment by an operator. He has only to switch on the 'block' button on the front panel of the logic controller. The injector is able to stay at this mode for a long time and it will start to work after switching off the 'block' button and initiating new cycle by an external pulse. To finish the injector operation, one should stop the cycle, open gate valves, switch off all fuel gas valves and the heaters inside the cryostat and the dewar vessel. After 30 minutes one should to switch off the vacuum pumping system, stretch the helium transfer tube out of injector and switch off the control rack.

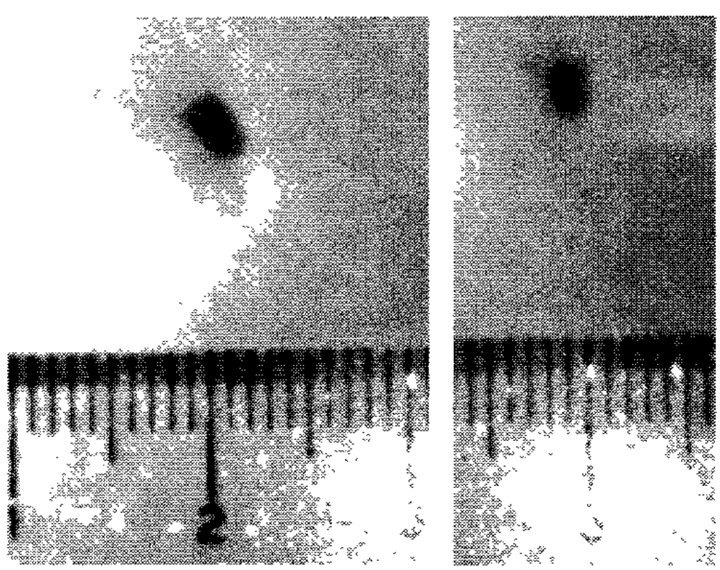

E104 E110

Fig. 11. Solid hydrogen pellets in flight at the injection rate of 1 shot per 5 s.

4. CONCLUSION

New repetitive pellet injector providing for a continuous injection of an unlimited number of pellets in steady-state mode is designed. The first stage of the injector testing is successfully completed. The innovative porous unit is developed to form and accelerate pellets for 5-9 s from every single barrel at the repetitive mode. As moving details, the injector has only fast valves for propellant gas admission in case of the pellet formation from solid fluid fuel, and gate valves extra in case of pellet formation from liquid fuel. This provides for high reliability of the long term injector operation. The injector requires only two-three pellets as a fuel reserve for a steady-state operation in comparison with an extruder injector, which contains hundreds of pellets. The injector design is compatible and attractive for the tritium operation. The aim of the second stage of the injector testing is to demonstrate the 5 Hz pellet injection with ten independently working barrels. A simulation and new porous unit design are developing now to reduce the pellet formation time to 1-2 s from every barrel also. The successful development and application of such injector allow to consider its as a technological machine for future refueling systems of fusion power stations.

5. ACKNOWLEDGMENTS

The authors would like to thank Professor A. Iiyoshi for his continuous encouragement. They are also grateful to K. Khlopenkov and S. Mizusawa of NIFS for their help with the pellet diagnostics and mechanical design and Prof. B. Kuteev, Dr. A. Umov, P. Koblents, V.Kapralov and Dr. S. Skoblikov of Applied Physics, LTD. for collaboration in the injector production. This research was sponsored by the National Institute for Fusion Science, Japan.

REFERENCES

[1] A. Iiyoshi, M. Fujiwara, O. Motojima, et al., Fusion Technology, 17, 1990, 169.

[2] I. Viniar, SU Patent 1611139 (1990). Russian Bulletin of the Discoveries and Inventories, 1997, No 15.

[3] I. Viniar and S. Sudo, NIFS report, NIFS-326, Dec 1994, 21.

[4] I. Viniar and S. Sudo, Rev. Sci. Instrum., 68(3), March 1997, 1444.

[5] S. Milora et al., Nucl. Fusion, 20, 1980, 1491.

[6] Y.Kamada et al., Nucl. Fusion, 29, 1989, 1785.

Recent Issues of NIFS Series

NIFS-456 G. Kawahara, S. Kida, M. Tanaka and S. Yanase,
Wrap, Tilt and Stretch of Vorticity Lines around a Strong Straight Vortex Tube in a Simple Shear Flow; Oct. 1996

NIFS-457 K. Itoh, S.- I. Itoh, A. Fukuyama and M. Yagi,
Turbulent Transport and Structural Transition in Confined Plasmas; Oct. 1996

NIFS-458 A. Kageyama and T. Sato,
Generation Mechanism of a Dipole Field by a Magnetohydrodynamic Dynamo; Oct. 1996

NIFS-459 K. Araki, J. Mizushima and S. Yanase,
The Non-axisymmetric Instability of the Wide-Gap Spherical Couette Flow; Oct. 1996

NIFS-460 Y. Hamada, A. Fujisawa, H. Iguchi, A. Nishizawa and Y. Kawasumi,
A Tandem Parallel Plate Analyzer; Nov. 1996

NIFS-461 Y. Hamada, A. Nishizawa, Y. Kawasumi, A. Fujisawa, K. Narihara, K. Ida, A. Ejiri, S. Ohdachi, K. Kawahata, K. Toi, K. Sato, T. Seki, H. Iguchi, K. Adachi, S. Hidekuma, S.Hirokura, K. Iwasaki, T. Ido, M. Kojima, J. Koong, R. Kumazawa, H. Kuramoto, T. Minami, I. Nomura, H. Sakakita, M. Sasao, K.N. Sato, T. Tsuzuki, J. Xu, I. Yamada and T. Watari,
Density Fluctuation in JIPP T-IIU Tokamak Plasmas Measured by a Heavy Ion Beam Probe; Nov. 1996

NIFS-462 N. Katsuragawa, H. Hojo and A. Mase,
Simulation Study on Cross Polarization Scattering of Ultrashort-Pulse Electromagnetic Waves; Nov. 1996

NIFS-463 V. Voitsenya, V. Konovalov, O. Motojima, K. Narihara, M. Becker and B. Schunke,
Evaluations of Different Metals for Manufacturing Mirrors of Thomson Scattering System for the LHD Divertor Plasma; Nov. 1996

NIFS-464 M. Pereyaslavets, M. Sato, T. Shimozuma, Y. Takita, H. Idei, S. Kubo, K. Ohkubo and K. Hayashi,
Development and Simulation of RF Components for High Power Millimeter Wave Gyrotrons; Nov. 1996

NIFS-465 V.S. Voitsenya, S. Masuzaki, O. Motojima, N. Noda and N. Ohyabu,
On the Use of CX Atom Analyzer for Study Characteristics of Ion Component in a LHD Divertor Plasma; Dec. 1996

NIFS-466 H. Miura and S. Kida,
Identification of Tubular Vortices in Complex Flows; Dec. 1996

NIFS-467 Y. Takeiri, Y. Oka, M. Osakabe, K. Tsumori, O. Kaneko, T. Takanashi, E. Asano, T.

Kawamoto, R. Akiyama and T. Kuroda,
Suppression of Accelerated Electrons in a High-current Large Negative Ion Source; Dec. 1996

NIFS-468 A. Sagara, Y. Hasegawa, K. Tsuzuki, N. Inoue, H. Suzuki, T. Morisaki, N. Noda, O. Motojima, S. Okamura, K. Matsuoka, R. Akiyama, K. Ida, H. Idei, K. Iwasaki, S. Kubo, T. Minami, S. Morita, K. Narihara, T. Ozaki, K. Sato, C. Takahashi, K. Tanaka, K. Toi and I. Yamada,
Real Time Boronization Experiments in CHS and Scaling for LHD; Dec. 1996

NIFS-469 V.L. Vdovin, T.Watari and A. Fukuyama,
3D Maxwell-Vlasov Boundary Value Problem Solution in Stellarator Geometry in Ion Cyclotron Frequency Range (final report); Dec. 1996

NIFS-470 N. Nakajima, M. Yokoyama, M. Okamoto and J. Nührenberg,
Optimization of M=2 Stellarator; Dec. 1996

NIFS-471 A. Fujisawa. H. Iguchi, S. Lee and Y. Hamada,
Effects of Horizontal Injection Angle Displacements on Energy Measurements with Parallel Plate Energy Analyzer; Dec. 1996

NIFS-472 R. Kanno, N. Nakajima, H. Sugama. M. Okamoto and Y. Ogawa,
Effects of Finite-β and Radial Electric Fields on Neoclassical Transport in the Large Helical Device; Jan. 1997

NIFS-473 S. Murakami, N. Nakajima, U. Gasparino and M. Okamoto,
Simulation Study of Radial Electric Field in CHS and LHD; Jan. 1997

NIFS-474 K. Ohkubo, S. Kubo, H. Idei, M. Sato, T. Shimozuma and Y. Takita,
Coupling of Tilting Gaussian Beam with Hybrid Mode in the Corrugated Waveguide; Jan. 1997

NIFS-475 A. Fujisawa, H. Iguchi, S. Lee and Y. Hamada,
Consideration of Fluctuation in Secondary Beam Intensity of Heavy Ion Beam Prove Measurements; Jan. 1997

NIFS-476 Y. Takeiri, M. Osakabe, Y. Oka, K. Tsumori, O. Kaneko, T. Takanashi, E. Asano, T. Kawamoto, R. Akiyama and T. Kuroda,
Long-pulse Operation of a Cesium-Seeded High-Current Large Negative Ion Source; Jan. 1997

NIFS-477 H. Kuramoto, K. Toi, N. Haraki, K. Sato, J. Xu, A. Ejiri, K. Narihara, T. Seki, S. Ohdachi, K. Adati, R. Akiyama, Y. Hamada, S. Hirokura, K. Kawahata and M. Kojima,
Study of Toroidal Current Penetration during Current Ramp in JIPP T-IIU with Fast Response Zeeman Polarimeter; Jan., 1997

NIFS-478 H. Sugama and W. Horton,
Neoclassical Electron and Ion Transport in Toroidally Rotating Plasmas; Jan. 1997

NIFS-479 V.L. Vdovin and I.V. Kamenskij,
3D Electromagnetic Theory of ICRF Multi Port Multi Loop Antenna; Jan. 1997

NIFS-480 W.X. Wang, M. Okamoto, N. Nakajima, S Murakami and N. Ohyabu,
Cooling Effect of Secondary Electrons in the High Temperature Divertor Operation; Feb. 1997

NIFS-481 K. Itoh, S.-I. Itoh, H. Soltwisch and H.R. Koslowski,
Generation of Toroidal Current Sheet at Sawtooth Crash; Feb. 1997

NIFS-482 K. Ichiguchi,
Collisionality Dependence of Mercier Stability in LHD Equilibria with Bootstrap Currents; Feb. 1997

NIFS-483 S. Fujiwara and T. Sato,
Molecular Dynamics Simulations of Structural Formation of a Single Polymer Chain: Bond-orientational Order and Conformational Defects; Feb. 1997

NIFS-484 T. Ohkawa,
Reduction of Turbulence by Sheared Toroidal Flow on a Flux Surface; Feb. 1997

NIFS-485 K. Narihara, K. Toi, Y. Hamada, K. Yamauchi, K. Adachi, I. Yamada, K. N. Sato, K. Kawahata, A. Nishizawa, S. Ohdachi, K. Sato, T. Seki, T. Watari, J. Xu, A. Ejiri, S. Hirokura, K. Ida, Y. Kawasumi, M. Kojima, H. Sakakita, T. Ido, K. Kitachi, J. Koog and H. Kuramoto,
Observation of Dusts by Laser Scattering Method in theJIPPT-IIU Tokamak Mar. 1997

NIFS-486 S. Bazdenkov, T. Sato and The Complexity Simulation Group,
Topological Transformations in Isolated Straight Magnetic Flux Tube; Mar. 1997

NIFS-487 M. Okamoto,
Configuration Studies of LHD Plasmas; Mar. 1997

NIFS-488 A. Fujisawa, H. Iguchi, H. Sanuki, K. Itoh, S. Lee, Y. Hamada, S. Kubo, H. Idei, R. Akiyama, K. Tanaka, T. Minami, K. Ida, S. Nishimura, S. Morita, M. Kojima, S. Hidekuma, S.-I. Itoh, C. Takahashi, N. Inoue, H. Suzuki, S. Okamura and K. Matsuoka,
Dynamic Behavior of Potential in the Plasma Core of the CHS Heliotron/Torsatron; Apr. 1997

NIFS-489 T. Ohkawa,
Pfirsch - Schlüter Diffusion with Anisotropic and Nonuniform Superthermal Ion Pressure; Apr. 1997

NIFS-490 S. Ishiguro and The Complexity Simulation Group, *Formation of Wave-front Pattern Accompanied by Current-driven Electrostatic Ion-cyclotron Instabilities*; Apr. 1997

NIFS-491 A. Ejiri, K. Shinohara and K. Kawahata,
An Algorithm to Remove Fringe Jumps and its Application to Microwave Reflectometry; Apr. 1997

NIFS-492 K. Ichiguchi, N. Nakajima, M. Okamoto,
Bootstrap Current in the Large Helical Device with Unbalanced Helical Coil Currents; Apr. 1997

NIFS-493 S. Ishiguro, T. Sato, H. Takamaru and The Complexity Simulation Group,
V-shaped dc Potential Structure Caused by Current-driven Electrostatic Ion-cyclotron Instability; May 1997

NIFS-494 K. Nishimura, R. Horiuchi, T. Sato,
Tilt Stabilization by Energetic Ions Crossing Magnetic Separatrix in Field-Reversed Configuration; June 1997

NIFS-495 T. -H. Watanabe and T. Sato,
Magnetohydrodynamic Approach to the Feedback Instability; July 1997

NIFS-496 K. Itoh, T. Ohkawa, S. -I.Itoh, M. Yagi and A. Fukuyama
Suppression of Plasma Turbulence by Asymmetric Superthermal Ions; July 1997

NIFS-497 T. Takahashi, Y. Tomita, H. Momota and Nikita V. Shabrov,
Collisionless Pitch Angle Scattering of Plasma Ions at the Edge Region of an FRC; July 1997

NIFS-498 M. Tanaka, A.Yu Grosberg, V.S. Pande and T. Tanaka,
Molecular Dynamics and Structure Organization in Strongly-Coupled Chain of Charged Particles; July 1997

NIFS-499 S. Goto and S. Kida,
Direct-interaction Approximation and Reynolds-number Reversed Expansion for a Dynamical System; July 1997

NIFS-500 K. Tsuzuki, N. Inoue, A. Sagara, N. Noda, O. Motojima, T. Mochizuki, T. Hino and T. Yamashina,
Dynamic Behavior of Hydrogen Atoms with a Boronized Wall; July 1997

NIFS-501 I. Viniar and S. Sudo,
Multibarrel Repetitive Injector with a Porous Pellet Formation Unit; July 1997